Applied Physics A (2018) 124:639
https://doi.org/10.1007/s00339-018-2062-y

Applied Physics A
Materials Science & Processing

Hopping conductivity-mediated O-shaped memory behaviour in gelatin–graphene oxide composite films

Sreedevi Vallabhapurapu[1,2] · Ashwini Rohom[3] · N. B. Chaure[3] · C. Tu[2] · S. Du[4] · V. V. Srinivasu[5] · Ananthakrishnan Srinivasan[5,6]

Received: 10 June 2018 / Accepted: 21 August 2018
© Springer-Verlag GmbH Germany, part of Springer Nature 2018

Abstract

Gelatin–graphene oxide composite films were prepared by spin coating graphene oxide (GO) dispersed in type-A gelatin on indium tin oxide (ITO) substrates. Current–voltage (*I–V*) characteristics of the composite film with Al as top electrode and ITO as bottom electrode, exhibited O-shaped memory behaviour. The influence of GO in the observed phenomenon was validated, when the *I–V* characteristics of pristine type-A gelatin film did not show any memory behaviour. Analysis of the forward and reverse *I–V* data leading to the ON and OFF states, respectively, revealed hopping type of conduction mechanism. We propose that formation and rupture of conducting filaments controlled by charge hopping mechanism leads to the observed low resistance (ON) and high resistance (OFF) states, respectively.

1 Introduction

Research on resistive random access memory (ReRAM) devices based on organic materials is gaining momentum in recent years [1–10]. This is because these materials offer high flexibility, easy solution-based processing, immense scope for miniaturisation, and tailored properties by appropriate choice of dispersant and matrix. There are many reports on successful improvement of memory performance in organic or polymer–nanocomposite-based ReRAM devices in the literature [7–11].

Current–voltage (*I–V*) characteristics of these resistive memory systems are classified into three types based on the shape of the curves as N-shaped, S-shaped and O-shaped [12]. Both N-shaped and S-shaped *I–V* characteristics exhibit a sudden jump in current at a threshold voltage; whereas O-shaped characteristics are devoid of such abrupt change in current at a particular voltage, but instead reveal a cyclic change in current resembling the alphabet 'O'. However, the phenomenon of resistive switching and the factors that control it are not fully understood.

Recently, memory-type behaviour has been observed in *I–V* characteristics of biomaterials like melanin, ferratin and certain enzymes [13–16]. Biodegradable materials are of great interest in the area of resistive switching memory applications because they are environmentally friendly and nontoxic. Gelatin is a biodegradable biomaterial with excellent film forming capability which can be produced by low-cost processes [17, 18].

Gelatin has already been identified as a potential candidate for ReRAM application [18]. High ON/OFF ratio of 10^6 has been reported in a simple ReRAM cell structure of Al/gelatin/ITO [18]. The authors attribute the switching mechanism to conducting filament formation and rupture in B-type gelatin. Depending on the source and processing involved, two types of gelatin, i.e., type-A and type-B are commonly available [19]. In this context, it is of relevance to test the universality of memory switching in different types of gelatin. It was reported that type-A gelatin film did not show

✉ V. V. Srinivasu
vallavs@unisa.ac.za

[1] School of Computing, University of South Africa, Johannesburg 1710, South Africa

[2] Computer Systems Engineering, Faculty of Information and Communication Technology, Tshwane University of Technology, Pretoria 0183, South Africa

[3] Department of Physics, Savitribai Phule Pune University, Pune 411007, India

[4] Department of Electrical Engineering, Faculty of Commerce and Built Environment, Tshwane University of Technology, Pretoria 0183, South Africa

[5] Department of Physics, University of South Africa, Johannesburg 1710, South Africa

[6] Department of Physics, Indian Institute of Technology Guwahati, Guwahati 781039, India

any switching behaviour and that CdTe quantum dots have to be added into the gelatin matrix, in order to observe any memory behaviour [20]. Apart from the zero-dimensional nano-particle (like CdTe quantum dots) addition in type-A gelatin, it is of great interest to see the role of 2D materials inclusions in gelatin for their electrical conduction and switching properties.

In recent times, 2D materials are sweeping the scientific interest because of their exceptional properties and device applications [21–24]. In an excellent review of 2D materials [21], it was emphasised that, the charge carriers can move easily in-plane but are confined along the thickness in 2D nanomaterials. 2D nanomaterials have high sensitivity to external stimuli due to their large planar area. This is an important characteristic suitable for a variety of applications, based on surface activity. Therefore, it is of great interest to incorporate 2D material like graphene or graphene oxide into a polymer matrix and to study the conduction behaviour and look for resistive switching. In fact addition of graphene oxide (GO) into PVA was able to bring in the resistive switching behaviour [25]. This motivated us to incorporate GO in type-A gelatin to achieve resistive switching memory behaviour. GO can be reduced locally by forming oxygen vacancies which can result in formation of conducting filaments. Hence, there is a possibility of obtaining memory-type behaviour by introducing GO in gelatin matrix. Inspired by this, we carried out detailed *I*–*V* measurements and analysis of conduction mechanisms of type-A gelatin films with and without GO dispersant.

2 Experimental

Type-A gelatin with Bloom strength of 300 and purity 99.5%, was purchased from Goodrich Ingredients and Chemicals Pvt Ltd, Chennai, India. Graphene oxide (GO, 4–10% edge oxidised, product code: 1002071346) and indium tin oxide (ITO) coated glass were procured from Sigma-Aldrich.

ITO-coated glass substrate was first cleaned using acetone, methanol and distilled water. Gelatin solution was prepared by dissolving 5 g of gelatin pieces in 100 ml of distilled water maintained at 50 °C under continuous stirring with a magnetic stirrer. Pristine gelatin device was fabricated by spin coating a few drops of gelatin solution on pre-cleaned ITO-coated glass. The rotation speed was 500 rpm for 15 s followed by 2500 rpm for 30 s. For fabricating gelatin–GO composite film, 50 mg and 100 mg GO were separately added to 10 ml of gelatin solution to form 0.5 and 1 wt/v% GO–gelatin mixtures, respectively. The mixtures were sonicated for 10 min to form homogeneous solutions. The two solutions were then spin coated on pre-cleaned ITO-coated glass. Again a rotation scheme of 500 rpm for 15 s followed by 2500 rpm at 30 s was followed to form gelatin–0.5 wt/v% GO and gelatin–1 wt/v% GO films on ITO. The films were then dried at room temperature.

Thickness of the films was estimated using Filmetrics F10 thin film analyzer. The thickness was ~643 nm for gelatin–0.5 wt/v% GO and ~843 nm for gelatin–1 wt/v% GO. Al top electrodes of area 0.5 cm^2 was thermally evaporated on all the films using a home-made thermal evaporator with a base pressure of 2×10^{-5} mbar. A scanning electron microscope (SEM, Jeol, JSM 6360 A) was employed to examine the surface morphology of the thin film layers and to confirm the homogeneity of the films. *I*–*V* measurements were performed at room temperature using a semiconductor parameter analyser (Keithley 4200-SCS).

3 Results and discussion

Figure 1 shows a schematic diagram of the device fabricated using the films and the measurement model. A typical SEM micrograph is shown in Fig. 2 for a spin-coated film with 0.5 wt% GO dispersed in type-A gelatin. One can see the dispersion is fairly uniform, but with micron-size cluster formation.

Figure 3 depicts the semi-logarithmic plot of current as a function of voltage measured in pristine type-A gelatin film sandwiched between Al and ITO electrodes. Figure 3 shows

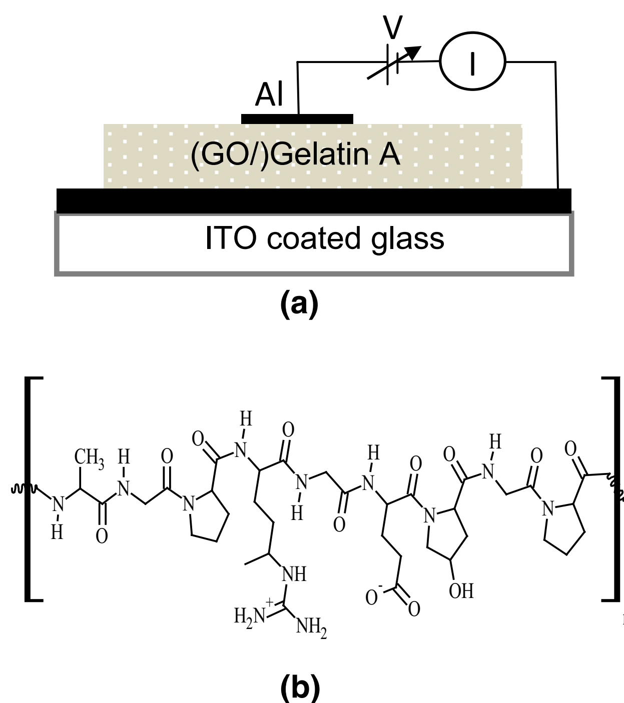

Fig. 1 **a** Structure of the ReRAM cell and the measurement scheme. **b** Representative structure of type-A gelatin

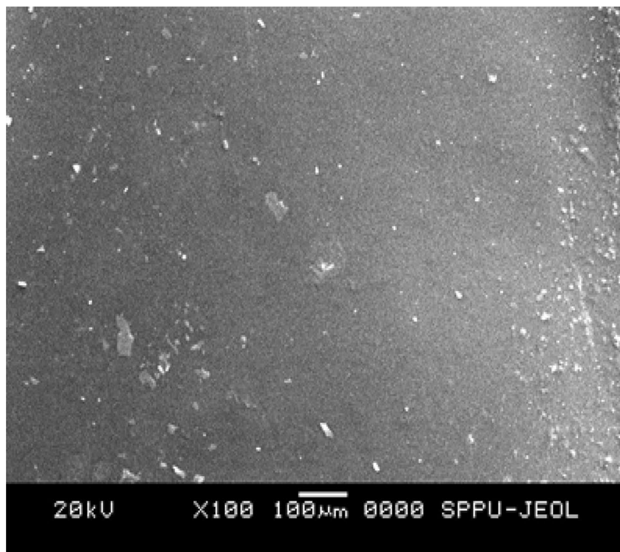

Fig. 2 Typical SEM micrograph of a 0.5 wt% GO-incorporated gelatin film

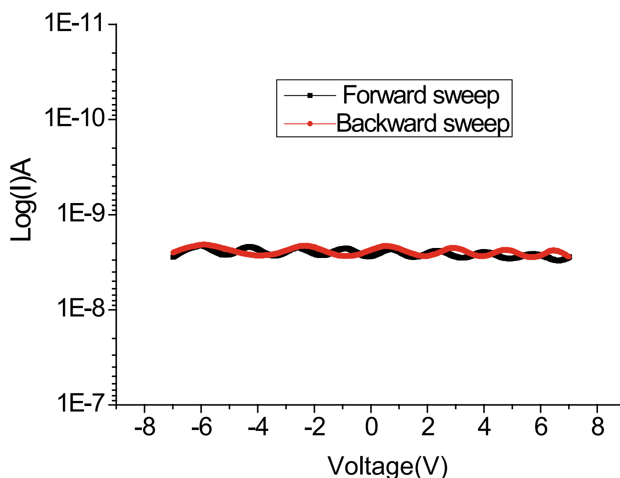

Fig. 3 *I–V* characteristics of the device fabricated with pristine gelatin film

the variation of current for voltage sweep from − 8 to + 8 V. The flat responses recorded on the forward and reverse sweeps clearly show that there is no resistive switching or any kind of hysteresis behaviour in the sample. This may be compared with the work of Chang and Wang [18] in which resistive switching was observed in type-B gelatin film sandwiched between Al and ITO electrodes. Absence of such switching behaviour in the highest Bloom strength type-A gelatin film with the same electrodes configuration indicate that this phenomenon may perhaps be limited to only type-B gelatin. It is obvious that the type-A gelatin film is incapable of generating conducting filaments under the influence of electric field to realise electrical conduction (switching) in the dielectric gelatin medium. Hence, it would be interesting to observe the role of GO (a 2-d allotrope of carbon) as dispersant in type-A gelatin. Figure 4 shows the *I–V* characteristics plotted on a semi-logarithmic scale for 0.5 wt% GO-incorporated gelatin film sandwiched between Al and ITO electrodes. It can be seen that the current decreases by nearly three orders of magnitude when the voltage is varied from − 8V to 0 V and then again rises back to the high current state when the voltage is increased to + 8V. Upon reversal of the voltage, the current goes to the lowest value at 0 V and again increases to high value at − 8 V. However, the current does not retrace its path in the reverse sweep. Such *I–V* characteristics represent the O-shaped hysteresis memory behaviour [12]. In this type of resistive memory behaviour, no abrupt increase of current at a specific voltage is observed. Here, the write voltage essentially either increases or decreases the electrical conductivity. This is qualitatively different from the S-shaped behaviour reported by Chang and Wang in pure type-B gelatin [18], where an abrupt increase or jump in current at a particular voltage was observed. Figure 5 shows the *I–V* characteristics plotted on a semi-logarithmic scale for 1 wt% GO-incorporated gelatin film sandwiched between Al and ITO electrodes which shows the same behaviour as the one displayed in Fig. 4. The presence of higher content of GO in this device is reflected in the larger change in the current. However, the distortion observed in the *I–V* indicates possible percolation of the graphene particles for higher GO content. In the case of GO-incorporated type-A gelatin, the ON/OFF ratio is smaller than the one reported in type-B gelatin film [18]. However, one cannot directly compare the two ON/OFF ratios since the switching mechanisms are entirely different in both the cases. So, the emphasis of this paper is on the analysis of this

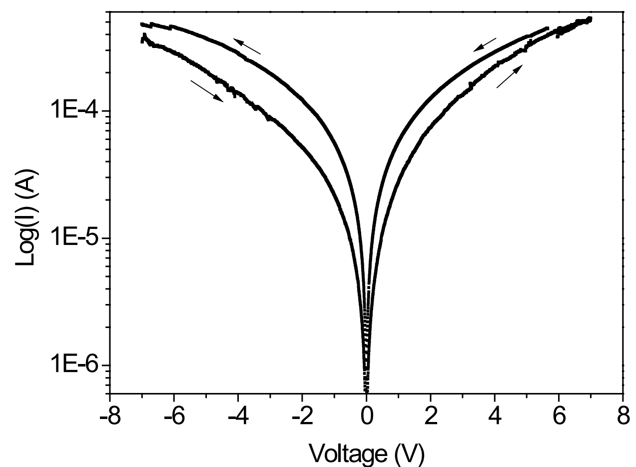

Fig. 4 Semi-logarithmic *I–V* plot obtained for the device with 0.5 wt% GO-incorporated gelatin film

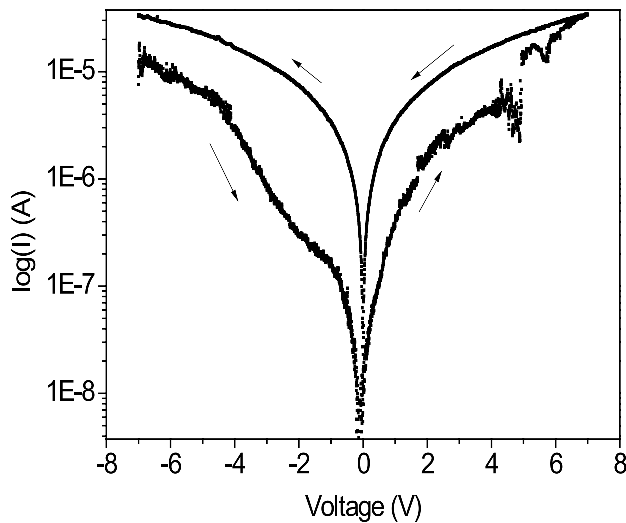

Fig. 5 Semi-logarithmic *I–V* plot obtained for the device with 1 wt% GO-incorporated gelatin film

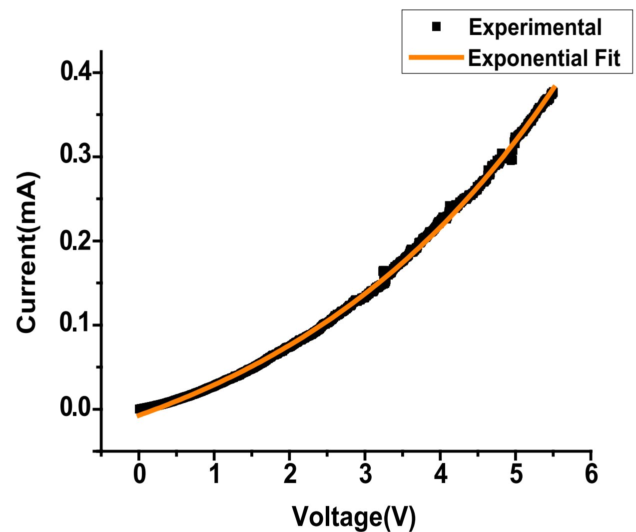

Fig. 6 *I–V* data for the OFF state of the device with 0.5 wt% GO-incorporated gelatin film. Solid line represents exponential fit to the experimental data

new type of memory behaviour observed for the first time in GO-incorporated type-A gelatin.

It is important to understand the conduction mechanisms involved in resistive switching memory systems [20, 25–31]. In most cases, in the low-voltage regime, one may have ohmic behaviour with $I \propto V^n$ with $n = 1$. And the thermionic emission behaviour with $n = 0.5$. At higher voltages, space charge limited conduction (SCLC) can dominate $n \sim 2$. However, there are cases when trap controlled space charge limited conduction can dominate in which case $n > 2$.

We examined various regions of the *I–V* data of the GO-incorporated type-A gelatin films in terms of different mechanisms such as ohmic, SCLC, etc. In the case of both the composite films, the *I–V* data showed $n \sim 1.5$ behaviour, ruling out both ohmic and SCLC-type conduction mechanisms. The data fitted very well with the expression representing hopping conductivity [32], with the current following the relation,

$$I = I_o + A\exp\{(V - V_a)/kT\}. \tag{1}$$

Here, I_o represents the residual current, the constant A is a product of mean hopping distance, number of electrons and thermal vibrational frequency of electrons at the trap. V_a is the characteristic voltage, when multiplied by the electronic charge gives the activation energy. k is the Boltzmann constant. Figures 6 and 7 show the exponential fits to the experimental data of 0.5 wt% GO-incorporated type-A gelatin device corresponding to the OFF and ON states, respectively. Good fits to Eq. (1) in the *I–V* data range covering both the ON and OFF states show that electron hopping is the only mechanism in these films. One can now understand the O-shaped hysteresis and bistable memory behaviour observed in the composite film devices as follows: it has been well established that application of electric field weakens the bonds between oxygen and graphene moves bridge site oxygen to top site, giving rise to domains of oxygen vacancies (V_o) and excess oxygen [33]. Electron can hop from electrode to V_o or V_o to V_o and then V_o to electrode, essentially forming a conduction filament through a hopping mechanism Then, according to Makarov et al. [31], formation of conduction filaments and the subsequent rupture

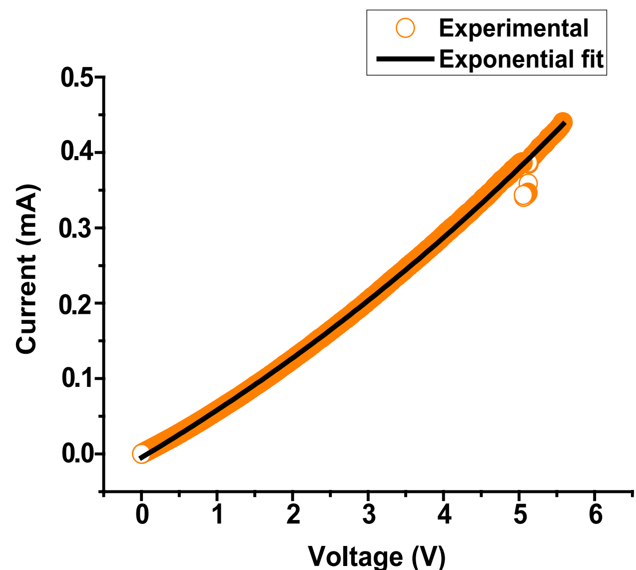

Fig. 7 *I–V* data for the ON state of the device with 0.5 wt% GO-incorporated gelatin film. Solid line represents exponential fit to the experimental data

of the same can lead to low resistance and high resistance states, respectively, and the hence the O-shaped behaviour.

We believe that increasing GO wt% from 0.5 to 1 may kick in percolation effects that can modify the conduction mechanism from pure hopping to hopping plus percolation. Hence, the optimum GO concentration is < 1 wt% for observing O-shaped memory effect in GO-incorporated type-A gelatin films. The conduction mechanism in gelatin–GO films is different from the other reported systems that show O-shaped memory behaviour such as PMMA:ZnO [29] and Ag-PMMA [34]. This shows that not all systems that exhibit O-shaped memory behaviour have the same type of conduction mechanism. Apart from the type of dispersant and the type of matrix, the concentration of the dispersant influences the conduction mechanism in these polymer–nanoparticle-based ReRAM materials.

4 Conclusion

Thin films of GO-incorporated type-A gelatin were prepared by simple spin-coating technique on ITO substrates. *I–V* characteristics of pristine type-A gelatin film shows no hysteresis or any sign of memory behaviour type unlike type-B gelatin films which shows S-type memory effect [18]. These rule out the universality of switching behaviour in all the types of pristine gelatin films. However, we observed O-shaped memory behaviour in GO-incorporated gelatin composite films. Analysis of conduction mechanism shows that a hopping-type conduction controlled conductive filament formation and rupture leads to bistability in these films. Compared with literature, we conclude that the conduction mechanism may not be the same for all systems showing the O-shaped memory behaviour.

Acknowledgements SV acknowledges partial financial support from the University of South Africa (UNISA). AS acknowledges a visiting professorship from UNISA and sabbatical leave from Indian Institute of Technology Guwahati.

References

1. B. Cho, S. Song, Y. Ji, T.-W. Kim, T. Lee, Adv. Funct. Mater. **21**, 2806–2829 (2011)
2. E. Guizzo, IEEE Spectr. **44**, 17–18 (2004)
3. Y. Yang, J. Ouyang, L. Ma, R.J.-H. Tseng, C.-W. Chu, Adv. Funct. Mater. **16**, 1001–1014 (2006)
4. W.P. Lin, S.J. Liu, T. Gong, Q. Zhao, W. Huang, Adv. Mater. **26**, 570–606 (2014)
5. D. Ma, M. Aguiar, J.A. Freire, I.A. Huemmelgen, Adv. Mater. **12**, 1063–1066 (2000)
6. Q.-D. Ling, D.-J. Liaw, E.Y.-H. Teo, C. Zhu, D.S.-H. Chan, E.-T. Kang, K.-G. Neoh, Polymer **48**, 5182–5201 (2007)
7. K. Onlaor, N. Chaithanatkun, B. Tunhoo, Curr. Appl. Phys. **16**, 1418–1423 (2016)
8. S. Valanarasu, A. Kathalingam, J.-K. Rhee, R. Chandramohan, T.A. Vijayan, M. Karunakaran, J. Nanosci. Nanotechnol. **15**(2), 1416–1420 (2015)
9. N.R. Hosseini, J.-S. Lee, Adv. Funct. Mater. **25**, 5586–5592 (2015)
10. A. Kathalingam, J.-K. Rhee, J. Electron. Mater. **41**, 2162–2168 (2012)
11. Y.-C. Chang, Y.-H. Wang, Appl. Phys. Lett. **106**, 123302 (2015)
12. D. Prime, S.P. Paul, Philos. Trans. R. Soc. A **367**, 4141–4157 (2009)
13. H. Baek, C. Lee, K. Lim, J. Cho, Nanotechnology **23**, 155604 (2012)
14. H. Baek, C. Lee, K. Lim, J. Park, Y. Kim, B. Koo, H. Shin, D. Wang, J. Cho, J. Mater. Chem. **22**, 4645–4651 (2012)
15. Y. Ko, Y. Kim, H. Baek, J. Cho, ACS Nano **5**, 9918–9926 (2011)
16. M. Ambrico, A. Cardone, T. Ligonzo, V. Augelli, P.F. Ambrico, S. Cicco, G.M. Farinola, M. Filannino, G. Perna, V. Capozzi, Org. Electron. **11**, 1809–1814 (2010)
17. M. Ramos, A. Valdés, A. Beltrán, M.C. Garrigós, Coatings **6**, 41 (2016)
18. Y.-C. Chang, Y.-H. Wang, ACS Appl. Mater. Interfaces **6**, 5413–5421 (2014)
19. P. Aramwit, N. Jaichawa, J. Ratanavaraporn, T. Srichana, Mater. Express **5**(3), 241–248 (2015)
20. S. Vallabhapurapu, A. Rohom, N.B. Chaure, S. Du, A. Srinivasan, AIP Conf. Proc. **1953**, 030271 (2018)
21. A.H. Khan, S. Ghosh, B. Pradhan, A. Dalui, L.K. Shrestha, S. Acharya, K. Ariga, Bull. Chem. Soc. Jpn. **90**, 627 (2017)
22. R. Frisenda, E. Navarro-Moratalla, P. Gant, D. Pe´rez, P. De Lara, R.V. Jarillo-Herrero, Gorbachev, A. Castellanos-Gomez, Chem. Soc. Rev. **47**, 53 (2018)
23. Y. Wang, C.C. Mayorga-Martinez, M. Pumera, Bull. Chem. Soc. Jpn. **90**, 847 (2017)
24. C. Tan, X. Cao, X.-J. Wu, Q. He, J. Yang, X. Zhang, J. Chen, W. Zhao, S. Han, G.-H. Nam, M. Sindoro, H. Zhang, Chem. Rev. **117**, 6225 (2017)
25. Y. Sun, J. Lu, C. Ai, D. Wen, Phys. Chem. Chem. Phys. **18**, 11341 (2016)
26. C. Ya-Peng, H. Yu-Feng, L. Jian-Tao, Y. Hai-Hang, L. Long-Feng, N. Yu, L. Qi-Peng, T. Ai-Wei, L. Zhi-Dong, H. Yan-Bing, T. Feng, Chin. Phys. B **24**, 037201 (2015)
27. A. Prakash, J. Ouyang, J.-L. Lin, Y. Yang, J. Appl. Phys. **100**, 054309 (2006)
28. J. Ouyang, C.-W. Chu, D. Sieves, Y. Yang, Appl. Phys. Lett. **86**, 123507 (2005)
29. B. Pradhan, S.K. Majee, S.K. Batabyal, A.J. Pal, J. Nanosci. Nanotechnol. **7**(12), 4534–4539 (2007)
30. J. Lin, D. Li, J.-S. Chen, J.-H. Li, D.-G. Ma, Chin. Phys. Lett. **24**(11), 3280–3282 (2007)
31. A. Makarov, V. Sverdlov, S. Selberherr, in *International Conference on Simulation of Semiconductor Processes and Devices, Bologna, Italy* (2010), pp. 237–240
32. F.-C. Chiu, Adv. Mater. Sci. Eng. **2014**, 578168 (2014)
33. M. Topsakal, H.H. Gürel, S. Ciraci, J. Phys. Chem. C **117**, 5943–5952 (2013)
34. B. Mukherjee, M. Mukherjee, Appl. Phys. Lett. **94**, 173510 (2009)